ACS APPLIED MATERIALS & INTERFACES

www.acsami.org

Research Article

Intrinsically Breathable and Flexible NO_2 Gas Sensors Produced by Laser Direct Writing of Self-Assembled Block Copolymers

Li Yang,* Huadong Ji, Chuizhou Meng, Yuhang Li, Guanghao Zheng, Xue Chen, Guangyu Niu, Jiayi Yan, Ye Xue, Shijie Guo,* and Huanyu Cheng*

Cite This: *ACS Appl. Mater. Interfaces* 2022, 14, 17818–17825

Read Online

ACCESS | Metrics & More | Article Recommendations | Supporting Information

ABSTRACT: The surge in air pollution and respiratory diseases across the globe has spurred significant interest in the development of flexible gas sensors prepared by low-cost and scalable fabrication methods. However, the limited breathability in the commonly used substrate materials reduces the exchange of air and moisture to result in irritation and a low level of comfort. This study presents the design and demonstration of a breathable, flexible, and highly sensitive NO_2 gas sensor based on the silver (Ag)-decorated laser-induced graphene (LIG) foam. The scalable laser direct writing transforms the self-assembled block copolymer and resin mixture with different mass ratios into highly porous LIG with varying pore sizes. Decoration of Ag nanoparticles on the porous LIG further increases the specific surface area and conductivity to result in a highly sensitive and selective composite to detect nitrogen oxides. The as-fabricated Ag/LIG gas sensor on a flexible polyethylene substrate exhibits a large response of −12‰, a fast response/recovery of 40/291 s, and a low detection limit of a few parts per billion at room temperature. Integrating the Ag/LIG composite on diverse fabric substrates further results in breathable gas sensors and intelligent clothing, which allows permeation of air and moisture to provide long-term practical use with an improved level of comfort.

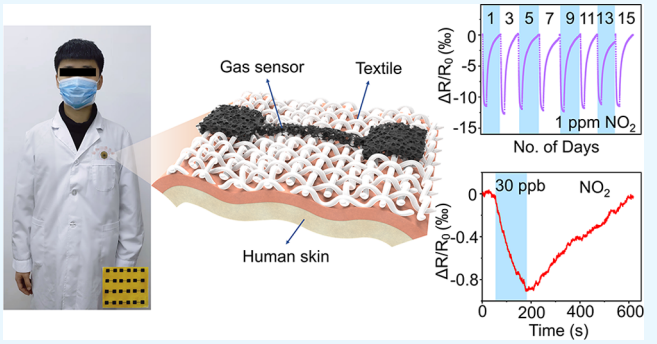

KEYWORDS: *scalable laser direct writing, self-assembled BCP/resin, Ag/LIG composites, intrinsically breathable and flexible gas sensors, intelligent clothing for gas sensing*

1. INTRODUCTION

Graphene-based nanomaterials have been widely used in flexible sensors and electronic devices due to their extremely high charge mobility, mechanical strength, and thermal conductivity.[1−3] However, the difficulty in large-area synthesis and integration presents challenges in device applications. Transient laser heating of various carbon-containing materials with a commercial laser is a cost-effective and scalable approach to generate functional porous materials such as laser-induced graphene (LIG).[4−7] However, it is challenging to achieve control of the pore size and the connectivity. Meanwhile, block copolymer (BCP) self-assembly has been explored to construct hierarchically porous nanoscale structures,[8] which find extensive applications in electrochemical sensors,[9−12] energy storage,[13−15] and electrothermal conversion.[16,17] As a result, coupling bottom-up BCP self-assembly with top-down laser direct writing has garnered high interest to rapidly produce the hierarchically porous materials.[18] The porous 3D structures with pore sizes easily modulated by the mass ratio of BCP to resins have been explored for microfluidics,[19] micro-batteries,[20,21] and supercapacitors.[22] However, their applications in gas sensing for biomarker detection from the human body or in the exposed environment are yet to be investigated.

As one representative example of the toxic air pollutants from the combustion of fossil fuel, nitrogen dioxide (NO_2) often causes adverse respiratory health problems such as irritation, chronic bronchitis, and emphysema.[23−25] While exposure to 10−20 ppm NO_2 is irritating, exposure to 150 ppm or higher may result in pulmonary edema or bronchospasm death.[26] There is also a possible link between long-term NO_2 exposure and mortality from heart failure and dysrhythmia.[27,28] Despite there being numerous gas sensors for detecting NO_2, their inflexibility and high operating temperature limit their future development.[29,30] Therefore, it is of increasing interest to develop wearable gas sensors for accurate and continuous recording of NO_2.[31−33] However, the limited

Received: February 2, 2022
Accepted: March 29, 2022
Published: April 8, 2022

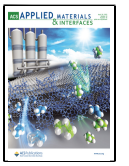

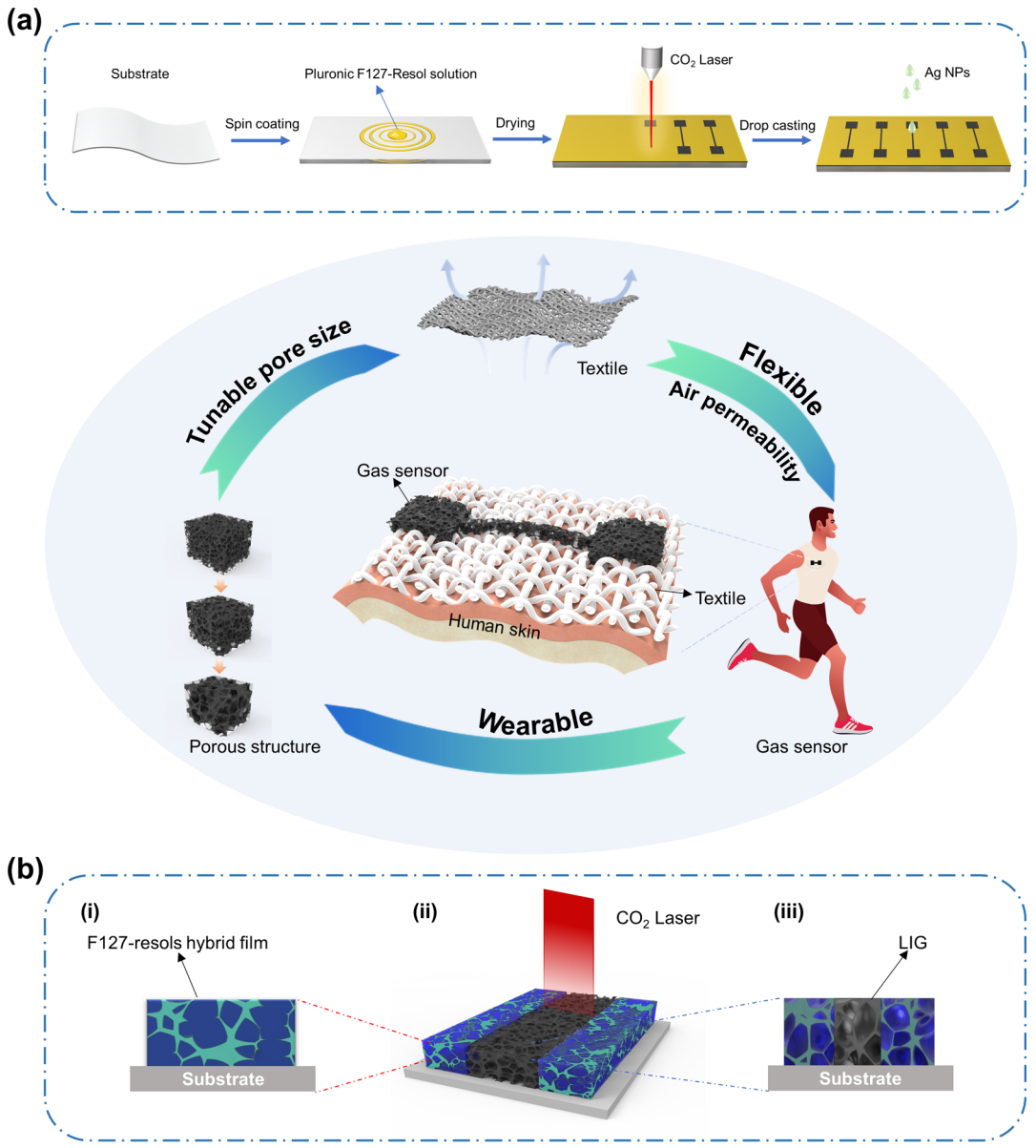

Figure 1. Schematic illustration showing the (a) fabrication process of the Ag/LIG-based breathable gas sensor that relies on the (b) transformation of F127/resols into porous LIG with transient heating by a CO_2 laser.

breathability of the commonly explored substrate materials on exposure to air and moisture often results in irritation and a reduced level of comfort during long-term use. The use of breathable textiles as the substrate in gas sensors allows them to detect NO_2,[34−36] ammonia,[37] hydrogen sulfide,[38] and volatile organic compounds.[39] Although simple dip-coating has been extensively explored,[40−42] the integration on wearable clothing requires sewing or an additional adhesive. The process is also incompatible with some commonly used textiles such as nylon and non-woven fabrics. Therefore, it is still challenging to fabricate breathable gas sensors on diverse fabric substrates.

Here, this work reports the design, fabrication, and demonstration of a breathable and flexible gas sensor on diverse substrates (e.g., polyethylene film, papers, and fabrics) by combining scalable laser direct writing with BCP/resin self-assembly. The self-assembled BCP/resin with varying mass ratios can be transformed into 3D porous LIG foam structures with tunable pore sizes and distributions by transient laser heating. The dependence of the pore size of the 3D porous graphene on the gas-sensing performance is systematically investigated. Decorating Ag nanoparticles (Ag NPs) on the porous LIG results in Ag/LIG composites with a high specific surface area for an enhanced gas-sensing response. The as-prepared Ag/LIG-based gas sensors on a flexible PET substrate exhibit a large response of −12‰, a fast response/recovery of 40/291 s, and a low detection limit of a few parts per billion at room temperature. Furthermore, replacing PET with the textile substrate provides breathable gas sensors and intelligent clothing for long-term practical gas-sensing.

2. EXPERIMENTAL SECTION

2.1. Materials. Phenol−formaldehyde resins (resols) purchased from Henan Boren Casting Material Co., Ltd. and Pluronic F127 copolymer [poly(ethylene oxide)-*block*-poly(propylene oxide)-*block*-poly(ethylene oxide)] purchased from Sigma-Aldrich were used as received. Ethanol was purchased from Suzhou Chenze Chemical Co., Ltd. Ag NPs (0.1 mg/mL) were purchased from XFNANO Materials Tech Co., Ltd.

https://doi.org/10.1021/acsami.2c02061
ACS Appl. Mater. Interfaces 2022, 14, 17818−17825

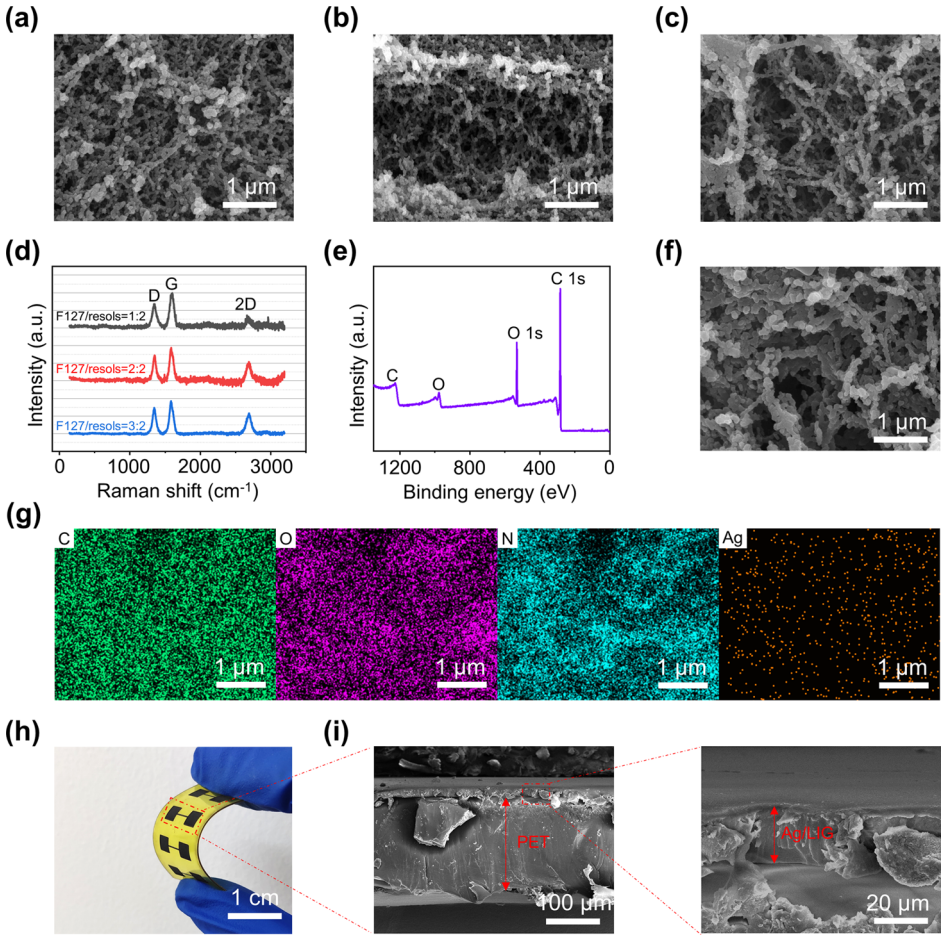

Figure 2. Characterization of the porous Ag/LIG composites. (a–c) SEM images of porous LIG structures prepared with varying mass ratios of Pluronic F127 to resols: (a) 1:2, (b) 2:2, and (c) 3:2. (d) Raman spectra in (a–c) and (e) XPS spectra of the LIG structure in (c). (f) SEM image of the LIG structure in (c) further coated with Ag nanoparticles. (g) Elemental mapping analyses of (f) for C, O, N, and Ag. (h) Optical image of Ag/LIG gas sensors on a flexible PET substrate, with (i) SEM images showing the cross section of the porous Ag/LIG composites.

2.2. Preparation of Self-Assembled BCP/Resol Hybrid Thin Films. The hybrid solution of BCP/resols was prepared by mixing the Pluronic F127 copolymer with resols in ethanol in a 40 °C water bath for 4 h. The F127/resol mass ratios were varied (i.e., 1:2, 2:2, and 3:2) to prepare three different samples. After vacuum degassing for 15 min, a two-step spin-coating with a low speed of 850 rpm for 15 s and a high-speed of 1500 rpm for 45 s was carried out to form a uniform hybrid thin film on the PET substrate, which was followed by curing in a vacuum oven at 150 °C for 2 h. When PET was replaced by the fabric substrates, the curing was performed at 100 °C for 12 h.

2.3. Fabrication and Testing of Breathable Gas Sensors. The gas sensor consisting of a straight sensing region (width of 300 μm, length of 5 mm) and two square electrode regions (Figure S1) was fabricated by transiently heating the hybrid BCP/resol thin films with a commercial CO_2 laser (Universal Laser, 10.6 μm) (Figure 1a). Fixed laser processing parameters were used unless specified otherwise: power of 2.4%, speed of 1%, and PPI of 500. After forming the 3D porous graphene with a programmed pattern in the hybrid film spin-coated on the diverse substrates (e.g., PET, paper, and fabric, Figure S2), drop-casting the Ag NPs on the LIG in the sensing region prepared the Ag/LIG composites for NO_2 detection. The connection between two square electrodes in the gas sensor and the data acquisition system was achieved by copper tapes with silver paste. The simple yet highly facile fabrication method directly and conveniently resulted in breathable gas sensors.

The sensing performance of the breathable gas sensors was characterized in a static gas testing system with a computer-controlled SourceMeter (Keithley 2400, Keithley Instruments, USA). Different concentrations of NO_2 in the sealed chamber with a volume of 10 L were prepared by diluting and mixing well the 100 ppm NO_2 calibration gas with air. The reading from the gas sensor was stabilized in static air for 60 s before testing. Testing of breathable gas sensors was performed under ambient conditions at room temperature.

2.4. Characterization. Scanning electron microscopy (SEM) images were collected using a field emission scanning electron microscope (JEOL, JSM 7100F). X-ray photoelectron spectroscopy (XPS) was performed using an ESCALAB 250 photoelectron spectrometer (Thermo Fisher Scientific, USA). Raman spectra were recorded using a laser micro Raman spectrometer (Renishaw, inVia Reflex). The electromechanical measurement of the breathable gas sensor was performed with the universal materials testing machine (JSV-H1000, Japan), whereas the sheet resistance was measured using a four-point probe.

3. RESULTS AND DISCUSSION

3.1. Characterization of 3D Porous Ag/LIG Composites. The design of breathable gas sensors relies on the simple and convenient creation of highly porous Ag/LIG composites on the textile substrate (Figure 1). In brief, the mixture of Pluronic F127 copolymer and resols spin-coated on the flexible substrate can be transiently heated using a CO_2 laser under ambient conditions to result in porous LIG with tunable pore sizes and distributions (Figure 1b). During laser scribing along the programmed pathway, the resols with a negative tone thermopolymerize into a continuous resin framework, whereas

https://doi.org/10.1021/acsami.2c02061
ACS Appl. Mater. Interfaces 2022, 14, 17818–17825

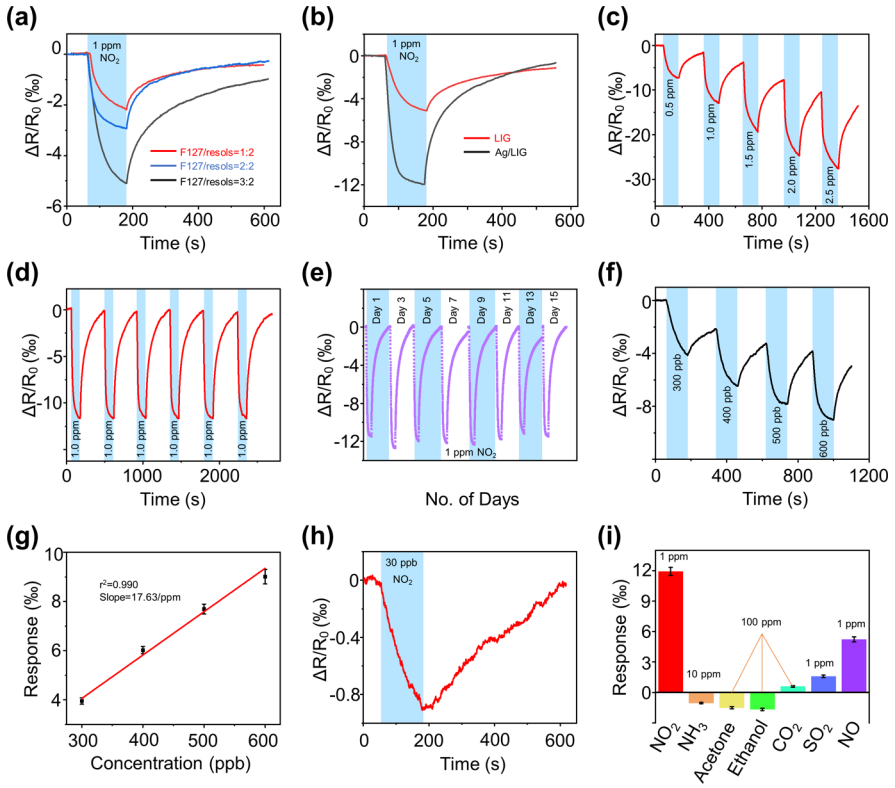

Figure 3. Evaluation of the gas-sensing performance of the as-prepared breathable sensor. The effects of the (a) F127/resol mass ratio and (b) decorated Ag NPs on a sensing response to 1 ppm NO_2. (c) Dynamic response of a Ag/LIG-based gas sensor upon exposure to NO_2 ranging from 0.5 to 2.5 ppm. (d) Repeatability test of the sensor to 1 ppm NO_2 over six cycles. (e) Stability demonstration of the gas sensor to 1 ppm NO_2 over 15 days. (f) Sensing response of the Ag/LIG-based gas sensor to parts per billion-level NO_2 with (g) its linear fitting. (h) Experimental demonstration of the gas sensor to detect 30 ppb NO_2. (i) Selectivity of the Ag/LIG-based gas sensor to NO_2 over ammonia, acetone, ethanol, CO_2, SO_2, and NO.

the BCP with a positive tone decomposes into a porous network, providing well-defined porous resin structures. The decoupled BCP breakdown from cross-linking of resols allows facile tuning of the porous structure by varying the mass ratio of Pluronic F127 to resols. As the mass ratio increases from 1:2 to 2:2 and then to 3:2, the average pore size in the 3D LIG increases from 100−150 to 200−300 nm (Figure 2a−c). The presence of few-layered porous graphene is confirmed by the three prominent peaks in the Raman spectrum: D peak (~1350 cm^{-1}), G peak (~1572 cm^{-1}), and 2D peak (~2697 cm^{-1}) (Figure 2d).[43] The chemical compositions of LIG revealed using XPS (Figure 2e) also show the deconvoluted C 1s into C−C (284.9 eV), C−O (285.8 eV), and C═O (288.3 eV) (Figure S3) to indicate the successful formation of graphene. Drop-casting Ag NPs on the 3D porous LIG (Figure 2f) further enhances the specific surface area and selective binding to the target gas molecules. The uniform distribution of Ag NPs on LIG is confirmed by the energy-dispersive spectroscopy (EDS) spectrum (Figures 2g and S4). The prepared Ag/LIG composites on diverse substrates (Figures 2h and S2) exhibit excellent flexibility (Figure 2i) and breathability. As the increase in the mass ratio of Pluronic F127 to resols from 1:2 to 2:2 and 3:2 results in 3D structures with a higher porosity and fewer conductive pathways, the resulting sample exhibits an increased sheet resistance from 28 to 32 and 41 sq^{-1} (size of 1 × 1 cm^2, Figure S5). The linear $I-V$ curves also indicate ohmic characteristics in the as-prepared samples (Figure S6).

3.2. Gas-Sensing Performance Characterization of Ag/LIG Composites. The performance of the Ag/LIG-based gas-sensing platform on diverse substrates (e.g., PET film, textile, and paper) is evaluated by exposing the sensor to NO_2 with a given concentration at room temperature for 120 s. After denoting R_0 and R_t as the resistance reading from the sensor in air and in the target gas, the gas sensor response defined as $S = (R_t - R_0)/R_0$ can be obtained for the porous LIG structure prepared by varying the F127/resol mass ratios on a flexible PET substrate (Figure 3a). The resistance reading from the sensor first decreases upon exposure to 1 ppm NO_2 and then recovers after returning the sensor back to the static air. The response time (τ_{resp}) and recovery time (τ_{recov}) are calculated as the time to reach 90% of total resistance change for NO_2 exposure and air re-exposure, respectively (Figure S7). The decreased resistance results from the increased hole density and electrical conductivity of the P-type LIG upon exposure to the oxidizing NO_2 (electron acceptor)[44,45] (Figure S8). As the F127/resol mass ratio increases from 1:2 to 3:2, the response in the absolute value increases from −2.3 to −5.1‰, which is likely attributed to the increased defects and adsorption sites as evidenced by the increased I_D/I_G ratio (Figure S9).[46,47] The larger pore size in LIG prepared by the higher F127/resol mass ratio may also expedite the adsorption rate of NO_2 molecules during the same exposure time for a larger gas response. The decoration of the Ag NPs, as confirmed by the binding energies of Ag $3d_{5/2}$ (368.3 eV) and Ag $3d_{3/2}$ (374.3 eV) in the XPS analysis[48] (Figure S10), on the porous LIG further enhances the sensor response by an

https://doi.org/10.1021/acsami.2c02061
ACS Appl. Mater. Interfaces 2022, 14, 17818−17825

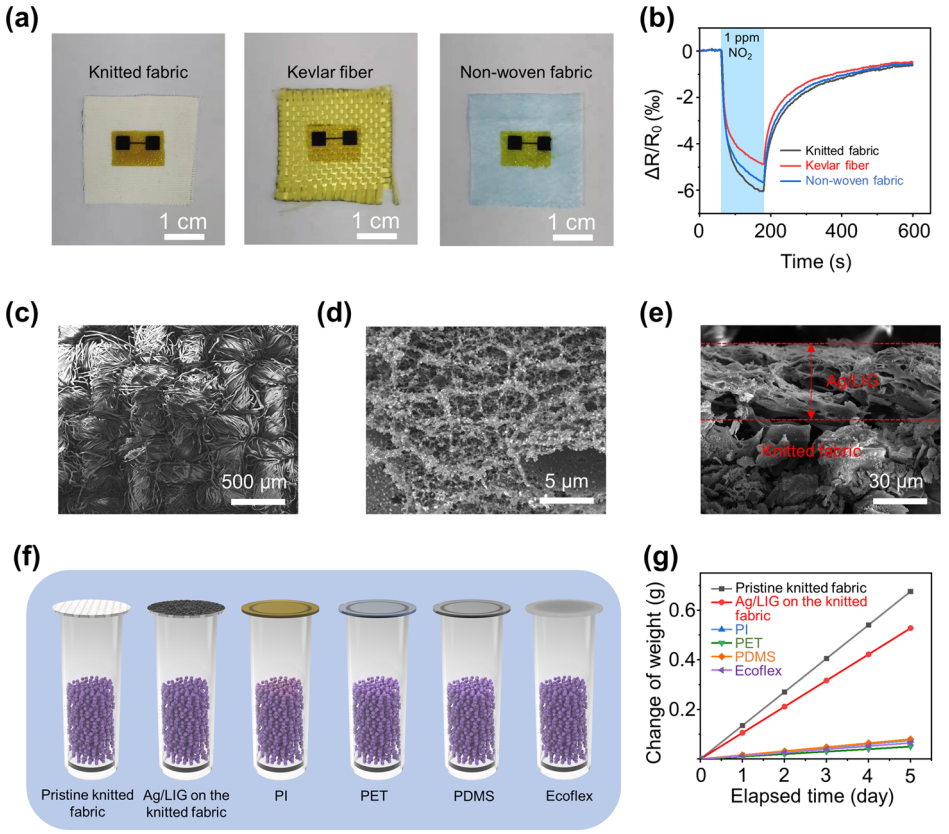

Figure 4. Characterizations of the Ag/LIG composites on the fabric substrate. (a) Optical images of Ag/LIG composites on knitted fabric, Kevlar fiber, non-woven fabric. (b) Response curves of the Ag/LIG-based gas sensors on different fabric substrates. SEM images of the knitted fabric (c) before and (d) after coating of Ag/LIG composites, with (e) the cross-sectional view of the Ag/LIG on the knitted fabric. (f) Experimental setup to measure the vapor transmission according to ASTM E96-95 and the (g) results on the change of weight with elapsed time.

approximately 2.4-fold increase (−12 vs −5.1‰, Figure 3b). The enhancement is likely attributed to the higher specific surface area and increased active sensing sites in the Ag/LIG composites.[49] Therefore, the Ag/LIG composite with the largest pore size prepared by the mass ratio of 3:2 is chosen in the following studies unless otherwise specified.

The Ag/LIG-based gas sensor is capable of detecting NO_2 from 0.5 to 2.5 ppm with a step size of 0.5 ppm to result in a response of −7.3, −12.5, −19.4, −24.7, and −27.6‰ (Figure 3c), demonstrating a relatively wide detection range. The sensor is also highly repeatable and stable over time, as evidenced by the almost unchanged response to 1 ppm NO_2 over six consecutive cycles (Figure 3d) and for 15 days (Figure 3e), demonstrating a high potential for practical applications. To calculate the theoretical limit of detection (LOD), the response of the Ag/LIG gas sensor to NO_2 with a progressively increasing concentration from 300 to 600 ppb is recorded (Figure 3f). The resulting linear fit of the response as a function of concentration provides a slope of 17.63 ppm^{-1} with a correlation coefficient (R^2) of 0.990 (Figure 3g). With RMS_{noise} as the standard deviation in the baseline response curve, the LOD = 3 × RMS_{noise}/slope[50] provides an estimation of the LOD to NO_2 as 6.5 ppb. In practical applications, the actual LOD often approximately corresponds to the signal with a signal-to-noise ratio (SNR) of 3 (SNR = $\Delta R/RMS_{noise}$). Although the sensor response to NO_2 is relatively small (e.g., −12‰ to 1 ppm NO_2), the SNR value of 691 from the ultralow noise level is still significantly higher than that of the other 2D nanomaterial-based gas sensors.[51] While it is challenging to directly validate the actual LOD with the static gas testing setup used in this work, the sensor to 30 ppb NO_2 still exhibits a steady response of −0.9‰ with an SNR of 61 (Figure 3h), implying the actual LOD to be close to sub-ppb level. The rapid response/recovery of 95/395 s is also observed at this ultralow concentration of NO_2. The excellent selectivity of the Ag/LIG-based gas sensor to NO_2 and NO is confirmed by its significantly larger response over a variety of other interfering gases, including ammonia (NH_3), acetone, ethanol, CO_2, and SO_2 (Figure 3i).

3.3. Demonstration of the Breathable Gas Sensor with Ag/LIG Composites on Fabrics. Preparing the Ag/LIG composites on diverse fabrics (e.g., knitted fabric, Kevlar fiber, non-woven fabric, and commercial clothes) results in an intrinsically breathable gas sensor (Figures 4a and S11). The breathable gas sensors on knitted fabric, Kevlar fabric, and non-woven fabric still exhibit large responses of −6.0, −5.5, and −5.1‰, respectively, with a fast response/recovery (65/405, 64/403, and 68/399 s) and high SNR values (351, 305, and 299) (Figure 4b, 1 ppm NO_2). The large detection range from 0.5 to 2.5 ppm is also confirmed in the dynamic response curves of the sensors on these three fabric substrates (Figure S12). The highest response for the sensor on the knitted fabric possibly comes from the largest adsorption surface area and most uniform coating on this natural fibrous structure (Figure 4c). The uniformly coated porous Ag/LIG composite on the knitted fabric surface (Figure 4d) maintains the inherent breathability of fabric (Figure 4e) to provide breathability in the resulting gas sensor. Per the ASTM E96-95 test,[52] the

https://doi.org/10.1021/acsami.2c02061
ACS Appl. Mater. Interfaces 2022, 14, 17818−17825

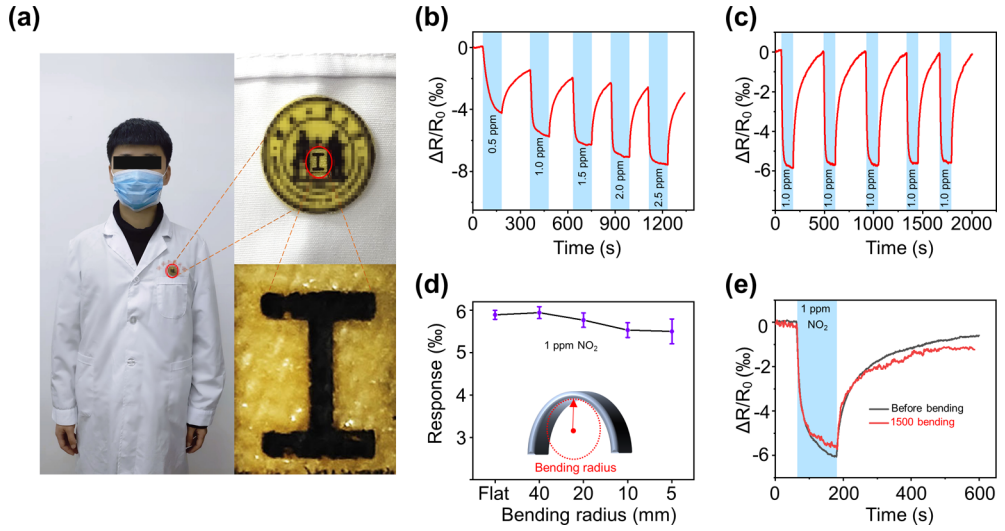

Figure 5. Intelligent lab coat based on the Ag/LIG composite gas sensor. (a) Optical images of the Ag/LIG composite on a lab coat with the university logo and the "I"-shaped Ag/LIG gas sensor shown in the insets. (b) Dynamic response of the Ag/LIG gas sensor on the knitted fabric to NO_2 with a concentration from 0.5 to 2.5 ppm. (c) Repeatability of the gas sensor to 1 ppm NO_2 over five consecutive cycles. (d) Stability of the gas sensor upon bending with varying bending radii of curvature (i.e., flat, 40, 20, 10, and 5 mm). (e) Comparison of the response of the gas sensor before and after 1500 bending cycles for a bending radius of curvature of 10 mm.

breathability is evaluated by measuring the weight change of the bottle covered by varying films with 20 g of silica gel desiccant inside (Figure 4f). With limited breathability when exposed to air and moisture, the bottles covered by conventional flexible elastomers such as PET, PI, PDMS, and Ecoflex films exhibit negligibly small weight changes. In contrast, the bottle covered by the Ag/LIG on the knitted fabric shows very close weight changes with that covered by the pristine knitted fabric, demonstrating an excellent vapor transmission rate (Figure 4g). Furthermore, the breathability of Ag/LIG composites on the knitted fabric can be easily controlled by tuning the pore size in the composite (Figure S13). The excellent breathability of Ag/LIG on the knitted fabric allows a rapid exchange of air and moisture between the human skin and the environment, which is highly desirable in wearable devices with an improved level of comfort for long-term use.

The excellent breathability of Ag/LIG on fabric provides a simple yet effective route to integrate the gas sensor on clothing such as lab coats to result in intelligent clothing (Figure 5a). The gas sensor on the intelligent coat lab shows large responses of −4.2, −5.8, −6.3, −7.1, and −7.6‰ to NO_2 as its concentration progressively increases from 0.5 to 2.5 ppm with a step size of 0.5 ppm (Figure 5b). The large response of −6‰ to 1 ppm NO_2 with a high SNR of 335 is also stable, with a small standard deviation of 1.4% over five consecutive cycles (Figure 5c). When the flexible sensor is subject to bending deformation with a radius of curvature (r) decreasing from 40 to 5 mm, the stable sensing response is also confirmed by the small standard deviation of 4.8% (Figure 5d). Taken together with the highly repeatable gas-sensing performance over 1500 bending cycles (Figure 5e), the breathable and flexible Ag/LIG on a fabric gas sensor opens up practical opportunities for long-term gas sensing with a significantly improved level of comfort. As a result, the Ag/LIG-based gas sensor with an ultralow LOD, a fast response/recovery, and an excellent vapor transmission rate from a tunable pore size compares favorably with other NO_2 gas sensors based on varying nanomaterials (Table S1).

4. CONCLUSIONS

In summary, we have reported the design, fabrication, and demonstration of a breathable, flexible, and highly sensitive NO_2 gas sensor based on Ag/LIG composites prepared by the simple yet scalable laser fabrication approach. The photothermal transformation of the self-assembled BCP/resols into highly porous 3D LIG foams with various pore sizes can be facilely achieved by laser direct writing with a tunable mass ratio of Pluronic F127 to resols. Drop-casting of Ag NPs onto the porous LIG surface further results in Ag/LIG composites with improved conductivity and specific surface area. The Ag/LIG-based gas sensor on the flexible PET substrate exhibits a large response of −12‰, a fast response/recovery of 40/291 s, and a low LOD of few parts per billion at room temperature. Replacing PET with the textile substrate results in intrinsically breathable and flexible gas sensors with a high sensitivity, a low LOD, and an excellent stability, which can allow the permeation of air and moisture for long-term sensing applications with an improved level of comfort.

■ ASSOCIATED CONTENT

Supporting Information

The Supporting Information is available free of charge at https://pubs.acs.org/doi/10.1021/acsami.2c02061.

Design and geometric parameters of the gas sensor; optical images of the F127/resols and corresponding LIG patterns (insets) on varying substrates; deconvoluted C 1s of the LIG prepared by the 3:2 F127/resols; SEM image of Ag-coated LIG (3:2 mass ratio) and the corresponding EDS spectrum; optical image of the four-point probe and the resulting sheet resistance measurements; current−voltage (I−V) curves of the LIG with three different F127/resol mass ratios; typical response curve of the pristine LIG gas sensor with the largest pore size to 1 ppm NO_2; schematic diagram showing the sensing mechanism of the Ag/LIG composite to NO_2; analysis of the peak intensity ratios of the D and 2D to G obtained from the Raman spectra; XPS analysis of the

https://doi.org/10.1021/acsami.2c02061
ACS Appl. Mater. Interfaces 2022, 14, 17818−17825

Ag 3d intensity in the Ag/LIG composite; optical images of the Ag/LIG composite on knitted fabric, Kevlar fiber, and non-woven fabric to demonstrate the large-scale production; dynamic response curves of a Ag/LIG-based gas sensor on three different fabric substrates upon exposure to NO_2 ranging from 0.5 to 2.5 ppm; and comparison in the weight change between the bottles covered by the knitted fabric and that with three different Ag/LIG composites (PDF)

AUTHOR INFORMATION

Corresponding Authors

Li Yang − *State Key Laboratory of Reliability and Intelligence of Electrical Equipment, School of Health Sciences and Biomedical Engineering, Hebei University of Technology, Tianjin 300130, China;* orcid.org/0000-0001-6798-3177; Email: yangli5781@126.com

Shijie Guo − *School of Mechanical Engineering, Hebei University of Technology, Tianjin 300130, China;* Email: guoshijie@hebut.edu.cn

Huanyu Cheng − *Department of Engineering Science and Mechanics, The Pennsylvania State University, University Park, Pennsylvania 16802, United States;* orcid.org/0000-0001-6075-4208; Email: huanyu.cheng@psu.edu

Authors

Huadong Ji − *School of Mechanical Engineering, Hebei University of Technology, Tianjin 300130, China*

Chuizhou Meng − *School of Mechanical Engineering, Hebei University of Technology, Tianjin 300130, China;* orcid.org/0000-0003-4266-3745

Yuhang Li − *Institute of Solid Mechanics, Beihang University (BUAA), Beijing 100191, China*

Guanghao Zheng − *School of Mechanical Engineering, Hebei University of Technology, Tianjin 300130, China*

Xue Chen − *School of Electrical Engineering, Hebei University of Technology, Tianjin 300130, China*

Guangyu Niu − *School of Architecture and Art Design, Hebei University of Technology, Tianjin 300130, China*

Jiayi Yan − *School of Mechanical Engineering, Hebei University of Technology, Tianjin 300130, China*

Ye Xue − *State Key Laboratory of Reliability and Intelligence of Electrical Equipment, School of Health Sciences and Biomedical Engineering, Hebei University of Technology, Tianjin 300130, China*

Complete contact information is available at: https://pubs.acs.org/10.1021/acsami.2c02061

Notes

The authors declare no competing financial interest.

ACKNOWLEDGMENTS

This work was supported by the National Natural Science Foundation of China (51705126, 61871173) and the Key Research and Development Project of Hebei Province (20271701D). H.C. acknowledges the supports provided by NSF (grant no. ECCS-1933072), NIH (award nos. R61HL154215 and R21EB030140), and the Penn State University.

REFERENCES

(1) Wang, B.; Ruan, T.; Chen, Y.; Jin, F.; Peng, L.; Zhou, Y.; Wang, D.; Dou, S. Graphene-Based Composites for Electrochemical Energy Storage. *Energy Storage Mater.* **2020**, *24*, 22−51.

(2) Yuan, W.; Shi, G. Graphene-based gas sensors. *J. Mater. Chem. A* **2013**, *1*, 10078−10091.

(3) Krishnan, S. K.; Singh, E.; Singh, P.; Meyyappan, M.; Nalwa, H. S. A Review on Graphene-Based Nanocomposites for Electrochemical and Fluorescent Biosensors. *RSC Adv.* **2019**, *9*, 8778−8881.

(4) Cao, L.; Zhu, S.; Pan, B.; Dai, X.; Zhao, W.; Liu, Y.; Xie, W.; Kuang, Y.; Liu, X. Stable and Durable Laser-Induced Graphene Patterns Embedded in Polymer Substrates. *Carbon* **2020**, *163*, 85−94.

(5) Chyan, Y.; Ye, R.; Li, Y.; Singh, S. P.; Arnusch, C. J.; Tour, J. M. Laser-Induced Graphene by Multiple Lasing: Toward Electronics on Cloth, Paper, and Food. *ACS Nano* **2018**, *12*, 2176−2183.

(6) Lin, J.; Peng, Z.; Liu, Y.; Ruiz-Zepeda, F.; Ye, R.; Samuel, E. L. G.; Yacaman, M. J.; Yakobson, B. I.; Tour, J. M. Laser-Induced Porous Graphene Films from Commercial Polymers. *Nat. Commun.* **2014**, *5*, 5714.

(7) Liu, J.; Zhang, L.; Yang, C.; Tao, S. Preparation of Multifunctional Porous Carbon Electrodes Through Direct Laser Writing on a Phenolic Resin Film. *J. Mater. Chem. A* **2019**, *7*, 21168−21175.

(8) Tan, K. W.; Wiesner, U. Block Copolymer Self-Assembly Directed Hierarchically Structured Materials from Nonequilibrium Transient Laser Heating. *Macromol* **2019**, *52*, 395−409.

(9) Duan, D.; Yang, H.; Ding, Y.; Li, L.; Ma, G. A Three-Dimensional Conductive Molecularly Imprinted Electrochemical Sensor Based on MOF Derived Porous Carbon/Carbon Nanotubes Composites and Prussian Blue Nanocubes Mediated Amplification for Chiral Analysis of Cysteine Enantiomers. *Electrochim. Acta* **2019**, *302*, 137−144.

(10) Zhang, Z.; Song, M.; Hao, J.; Wu, K.; Li, C.; Hu, C. Visible Light Laser-Induced Graphene from Phenolic Resin: A New Approach for Directly Writing Graphene-Based Electrochemical Devices on Various Substrates. *Carbon* **2018**, *127*, 287−296.

(11) Li, F.; Li, R.; Feng, Y.; Gong, T.; Zhang, M.; Wang, L.; Meng, T.; Jia, H.; Wang, H.; Zhang, Y. Facile Synthesis of Au-Embedded Porous Carbon from Metal-Organic Frameworks and for Sensitive Detection of Acetaminophen in Pharmaceutical Products. *Mater. Sci. Eng., C* **2019**, *95*, 78−85.

(12) Xu, G.; Jarjes, Z. A.; Desprez, V.; Kilmartin, P. A.; Travas-Sejdic, J. Sensitive, Selective, Disposable Electrochemical Dopamine Sensor Based on PEDOT-Modified Laser Scribed Graphene. *Biosens. Bioelectron.* **2018**, *107*, 184−191.

(13) Jayaramulu, K.; Dubal, D. P.; Nagar, B.; Ranc, V.; Tomanec, O.; Petr, M.; Datta, K. K. R.; Zboril, R.; Gómez-Romero, P.; Fischer, R. A. Ultrathin Hierarchical Porous Carbon Nanosheets for High-Performance Supercapacitors and Redox Electrolyte Energy Storage. *Adv. Mater.* **2018**, *30*, 1705789.

(14) Yan, J.; Miao, L.; Duan, H.; Zhu, D.; Lv, Y.; Xiong, W.; Li, L.; Gan, L.; Liu, M. Core-Shell Hierarchical Porous Carbon Spheres with N/O Doping for Efficient Energy Storage. *Electrochim. Acta* **2020**, *358*, 136899.

(15) Zhang, H.; Liu, Q.; Fang, Y.; Teng, C.; Liu, X.; Fang, P.; Tong, Y.; Lu, X. Boosting Zn-Ion Energy Storage Capability of Hierarchically Porous Carbon by Promoting Chemical Adsorption. *Adv. Mater.* **2019**, *31*, 1904948.

(16) Li, A.; Dong, C.; Dong, W.; Yuan, F.; Gao, H.; Chen, X.; Chen, X. B.; Wang, G. Network Structural CNTs Penetrate Porous Carbon Support for Phase-Change Materials with Enhanced Electro-Thermal Performance. *Adv. Electron. Mater.* **2020**, *6*, 1901428.

(17) Li, D.; Tang, B.; Lu, X.; Chen, W.; Dong, X.; Wang, J.; Wang, X. Hierarchically Carbonized Silk/Ceramic Composites for Electro-Thermal Conversion. *Composites, Part A* **2021**, *141*, 106237.

(18) Tan, K. W.; Jung, B.; Werner, J. G.; Rhoades, E. R.; Thompson, M. O.; Wiesner, U. Transient Laser Heating Induced Hierarchical Porous Structures from Block Copolymer-Directed Self-Assembly. *Science* **2015**, *349*, 54−58.

(19) Tan, Z.; Lan, W.; Liu, Q.; Wang, K.; Hussain, M.; Ren, M.; Geng, Z.; Zhang, L.; Luo, X.; Zhang, L.; Zhu, J. Kinetically Controlled Self-Assembly of Block Copolymers into Segmented Wormlike Micelles in Microfluidic Chips. *Langmuir* **2018**, *35*, 141−149.
(20) Tait, W. R. T.; Thedford, R. P.; Chapman, D. V.; Yu, F.; Freidl, J. W.; Sablina, E. S.; Batsimm, G. M.; Wiesner, U. B. One-Pot Structure Direction of Large-Pore Co-Continuous Carbon Monoliths from Ultralarge Linear Diblock Copolymers. *Chem. Mater.* **2021**, *33*, 7731−7742.
(21) Werner, J. G.; Rodríguez-Calero, G. G.; Abruña, H. D.; Wiesner, U. Block Copolymer Derived 3-D Interpenetrating Multifunctional Gyroidal Nanohybrids for Electrical Energy Storage. *Energy Environ. Sci.* **2018**, *11*, 1261−1270.
(22) Liu, T.; Liu, G. Block Copolymer-Based Porous Carbons for Supercapacitors. *J. Mater. Chem. A* **2019**, *7*, 23476−23488.
(23) Edginton, S.; O'Sullivan, D. E.; King, W. D.; Lougheed, M. D. The Effect of Acute Outdoor Air Pollution on Peak Expiratory Flow in Individuals with Asthma: A Systematic Review and Meta-Analysis. *Environ. Res.* **2021**, *192*, 110296.
(24) Guo, L.; Hao, Y.-W.; Li, P.-L.; Song, J.-F.; Yang, R.-Z.; Fu, X.-Y.; Xie, S.-Y.; Zhao, J.; Zhang, Y.-L. Improved NO_2 Gas Sensing Properties of Graphene Oxide Reduced by Two-Beam-Laser Interference. *Sci. Rep.* **2018**, *8*, 4918.
(25) Agrawal, A. V.; Kumar, R.; Venkatesan, S.; Zakhidov, A.; Yang, G.; Bao, J.; Kumar, M.; Kumar, M. Photoactivated Mixed In-Plane and Edge-Enriched P-Type MoS_2 Flake-Based NO_2 Sensor Working at Room Temperature. *ACS Sens.* **2018**, *3*, 998−1004.
(26) Yi, N.; Shen, M.; Erdely, D.; Cheng, H. Stretchable gas sensors for Detecting Biomarkers from Humans and Exposed Environments. *TrAC, Trends Anal. Chem.* **2020**, *133*, 116085.
(27) Ogen, Y. Assessing Nitrogen Dioxide (NO_2) Levels as A Contributing Factor to Coronavirus (COVID-19) Fatality. *Sci. Total Environ.* **2020**, *726*, 138605.
(28) Khan, H.; Zavabeti, A.; Wang, Y.; Harrison, C. J.; Carey, B. J.; Mohiuddin, M.; Chrimes, A. F.; De Castro, I. A.; Zhang, B. Y.; Sabri, Y. M.; Bhargava, S. K.; Ou, J. Z.; Daeneke, T.; Russo, S. P.; Li, Y.; Kalantar-zadeh, K. Quasi Physisorptive Two Dimensional Tungsten Oxide Nanosheets with Extraordinary Sensitivity and Selectivity to NO_2. *Nanoscale* **2017**, *9*, 19162−19175.
(29) Wang, X.; Sun, F.; Duan, Y.; Yin, Z.; Luo, W.; Huang, Y.; Chen, J. Highly Sensitive, Temperature-Dependent Gas Sensor based on Hierarchical ZnO Nanorod Arrays. *J. Mater. Chem. C* **2015**, *3*, 11397−11405.
(30) Wang, X.; Sun, F.; Huang, Y.; Duan, Y.; Yin, Z. A Patterned ZnO Nanorod Array/Gas Sensor Fabricated by Mechanoelectrospinning-Assisted Selective Growth. *Chem. Commun.* **2015**, *51*, 3117−3120.
(31) Singh, E.; Meyyappan, M.; Nalwa, H. S. Flexible Graphene-Based Wearable Gas and Chemical Sensors. *ACS Appl. Mater. Interfaces* **2017**, *9*, 34544−34586.
(32) Zheng, X.; Cheng, H. Flexible and Stretchable Metal Oxide Gas Sensors for Healthcare. *Sci. China Technol. Sci.* **2019**, *62*, 209−223.
(33) Yi, N.; Cheng, Z.; Li, H.; Yang, L.; Zhu, J.; Zheng, X.; Chen, Y.; Liu, Z.; Zhu, H.; Cheng, H. Stretchable, Ultrasensitive, and Low-Temperature NO_2 Sensors based on MoS_2@rGO Nanocomposites. *Mater. Today Phys.* **2020**, *15*, 100265.
(34) Doan, T. H. P.; Ta, Q. T. H.; Sreedhar, A.; Hang, N. T.; Yang, W.; Noh, J.-S. Highly Deformable Fabric Gas Sensors Integrating Multidimensional Functional Nanostructures. *ACS Sens.* **2020**, *5*, 2255−2262.
(35) Li, W.; Chen, R.; Qi, W.; Cai, L.; Sun, Y.; Sun, M.; Li, C.; Yang, X.; Xiang, L.; Xie, D.; Ren, T. Reduced Graphene Oxide/Mesoporous ZnO NSs Hybrid Fibers for Flexible, Stretchable, Twisted, and Wearable NO_2 E-Textile Gas Sensor. *ACS Sens.* **2019**, *4*, 2809−2818.
(36) Wang, H.; Wang, H.; Wang, Y.; Su, X.; Wang, C.; Zhang, M.; Jian, M.; Xia, K.; Liang, X.; Lu, H.; Li, S.; Zhang, Y. Laser Writing of Janus Graphene/Kevlar Textile for Intelligent Protective Clothing. *ACS Nano* **2020**, *14*, 3219−3226.
(37) Su, P.-G.; Liao, Z.-H. Fabrication of a Flexible Single-Yarn NH_3 Gas Sensor by Layer-By-Layer Self-Assembly of Graphene Oxide. *Mater. Chem. Phys.* **2019**, *224*, 349−356.
(38) Zhang, X.; Hao, X.; Zhai, Z.; Wang, J.; Li, H.; Sun, Y.; Qin, Y.; Niu, B.; Li, C. Flexible H_2S Sensors: Fabricated by Growing NO_2-Uio-66 on Electrospun Nanofibers for Detecting Ultralow Concentration H_2S. *Appl. Surf. Sci.* **2022**, *573*, 151446.
(39) Subbiah, D. K.; Mani, G. K.; Babu, K. J.; Das, A.; Balaguru Rayappan, J. B. Nanostructured ZnO on Cotton Fabrics − A Novel Flexible Gas Sensor & UV Filter. *J. Clean. Prod.* **2018**, *194*, 372−382.
(40) Ju Yun, Y.; Hong, W. G.; Choi, N.-J.; Hoon Kim, B.; Jun, Y.; Lee, H.-K. Ultrasensitive and Highly Selective Graphene-Based Single Yarn for Use in Wearable Gas Sensor. *Sci. Rep.* **2015**, *5*, 10904.
(41) Lee, S. W.; Lee, W.; Kim, I.; Lee, D.; Park, D.; Kim, W.; Park, J.; Lee, J. H.; Lee, G.; Yoon, D. S. Bio-Inspired Electronic Textile Yarn-Based NO_2 Sensor Using Amyloid−Graphene Composite. *ACS Sens.* **2021**, *6*, 777−785.
(42) Kim, D.; Keum, K.; Lee, G.; Kim, D.; Lee, S.-S.; Ha, J. S. Flexible, Water-Proof, Wire-Type Supercapacitors Integrated with Wire-Type UV/NO_2 Sensors on Textiles. *Nano Energy* **2017**, *35*, 199−206.
(43) Ferrari, A. C.; Meyer, J. C.; Scardaci, V.; Casiraghi, C.; Lazzeri, M.; Mauri, F.; Piscanec, S.; Jiang, D.; Novoselov, K. S.; Roth, S.; Geim, A. K. Raman Spectrum of Graphene and Graphene Layers. *Phys. Rev. Lett.* **2006**, *97*, 187401.
(44) Park, J.; Kim, Y.; Park, S. Y.; Sung, S. J.; Jang, H. W.; Park, C. R. Band Gap Engineering of Graphene Oxide for Ultrasensitive NO_2 Gas Sensing. *Carbon* **2020**, *159*, 175−184.
(45) Yang, L.; Yi, N.; Zhu, J.; Cheng, Z.; Yin, X.; Zhang, X.; Zhu, H.; Cheng, H. Novel Gas Sensing Platform Based on a Stretchable Laser-Induced Graphene Pattern with Self-Heating Capabilities. *J. Mater. Chem. A* **2020**, *8*, 6487−6500.
(46) Jung, W. T.; Jang, H.-S.; Jeon, J. W.; Kim, B. H. Effect of Oxygen Functional Groups in Reduced Graphene Oxide-Coated Silk Electronic Textiles for Enhancement of NO_2 Gas-Sensing Performance. *ACS Omega* **2021**, *6*, 27080−27088.
(47) Yan, W.; Yan, W.; Chen, T.; Xu, J.; Tian, Q.; Ho, D. Size-Tunable Flowerlike MoS_2 Nanospheres Combined with Laser-Induced Graphene Electrodes for NO_2 Sensing. *ACS Appl. Nano Mater.* **2020**, *3*, 2545−2553.
(48) Shao, W.; Liu, X.; Min, H.; Dong, G.; Feng, Q.; Zuo, S. Preparation, Characterization, and Antibacterial Activity of Silver Nanoparticle-Decorated Graphene Oxide Nanocomposite. *ACS Appl. Mater. Interfaces* **2015**, *7*, 6966−6973.
(49) Li, W.; Qi, W.; Cai, L.; Li, C.; Sun, Y.; Sun, M.; Yang, X.; Xiang, L.; Xie, D.; Ren, T. Enhanced Room-Temperature NO_2-Sensing Performance of AgNPs/rGO Nanocomposites. *Chem. Phys. Lett.* **2020**, *738*, 136873.
(50) Currie, L. A. Nomenclature in Evaluation of Analytical Methods Including Detection and quantification Capabilities (IUPAC Recommendations 1995). *Pure Appl. Chem.* **1995**, *67*, 1699−1723.
(51) Kim, S. J.; Koh, H.-J.; Ren, C. E.; Kwon, O.; Maleski, K.; Cho, S.-Y.; Anasori, B.; Kim, C.-K.; Choi, Y.-K.; Kim, J.; Gogotsi, Y.; Jung, H.-T. Metallic $Ti_3C_2T_x$ MXene Gas Sensors with Ultrahigh Signal-to-Noise Ratio. *ACS Nano* **2018**, *12*, 986−993.
(52) Jang, K.-I.; Han, S. Y.; Xu, S.; Mathewson, K. E.; Zhang, Y.; Jeong, J.-W.; Kim, G.-T.; Webb, R. C.; Lee, J. W.; Dawidczyk, T. J.; Kim, R. H.; Song, Y. M.; Yeo, W.-H.; Kim, S.; Cheng, H.; Rhee, S. I.; Chung, J.; Kim, B.; Chung, H. U.; Lee, D.; Yang, Y.; Cho, M.; Gaspar, J. G.; Carbonari, R.; Fabiani, M.; Gratton, G.; Huang, Y.; Rogers, J. A. Rugged and Breathable Forms of Stretchable Electronics with Adherent Composite Substrates for Transcutaneous Monitoring. *Nat. Commun.* **2014**, *5*, 4779.

https://doi.org/10.1021/acsami.2c02061
ACS Appl. Mater. Interfaces 2022, 14, 17818−17825